Targeted Cleavage of 16S Ribosomal RNA of *Escherichia coli* by Metallopeptides.

Research Thesis

Presented in partial fulfillment of the requirements for graduation *with Research Distinction* in Chemistry in the undergraduate colleges of The Ohio State University

by

Kevin Keuper

The Ohio State University

June 2012

Project Advisor: Professor James A. Cowan, Department of Chemistry

Acknowledgements

I would like to thank my mentor Jeff Joyner for guiding me through my project, as well as teaching me the basics and standards of scientific research. I would also like to thank Jeff for allowing me to use his program MassDaddy to help perform mass spectrometry analysis within a reasonable time frame.

I would also like to thank my project advisor James A. Cowan for helping keep me focused on the important things throughout my work and for guiding my research to display a more complete picture.

I would also like to thank my friends and family for supporting me, and also the Cowan Group for all of their contributions to help with this work.

Abstract

Copper was bound to modified peptides that selectively target the 16S ribosomal RNA of *Escherichia Coli* (*E. Coli*) and contain an amino terminal copper and nickel binding motif; and subsequent RNA cleavage studied. The metallopeptides (shown in Figure 1) Cu-GGHHPVHHYQ, Cu-GGHGHPVHHYQ, Cu-GGHGGHPVHHYQ, Cu-GGHGWRWYCR, and Cu-GGHGLPLTPLP were able to effectively transport the reactive metal center to the Fl-16S-rRNA to perform cleavage reactions. Initial cleavage rates were analyzed by polyacrilamide gel electrophoresis (PAGE) and found to be up to 120 nM/min with coreagents H_2O_2 and ascorbate, up to 2 nM/min with ascorbate, and up to 2.4 nM/min with no reagents. Matrix assisted laser desorption/ionization- time of flight mass spectrometry (MALDI-TOF MS) was used to detect RNA cleavage fragments with 6 easily identifiable nascent overhangs; 3'-hydroxyl , 2',3'-cyclic phosphate, 3'-phosphate, 3'-phosphoglycolate, 5'-hydroxyl, and 5'-phosphate at specific sites along the RNA sequence. Apparent initial rates of reaction were also determined from MALDI-TOF MS that were generally agreeable with initial rates determined by PAGE. The program MassDaddy (Jeff Joyner) was used to analyze mass spectra by comparing observed mass peaks to expected mass lists for cleavage products within a mass matching error of 200 ppm. This series of metallopeptides, with special focus on the hydrolytic cleavage shown by GGHGWRWYCR, shows promise in being able to target the 16S ribosomal RNA of *E. Coli* and function as an antibacterial drug.

Introduction

Antibacterial drugs are a major topic of study due to the slowly growing populations of antibiotic-resistant bacteria. Antibiotics have been in use for over 60 years, and it is becoming more common for antibiotic-resistant bacteria to infect humans. For example, shiga toxin-producing *E. Coli* can cause haemorrhagic colitis and haemolytic uraemic syndrome in the intestine and cannot be treated with most antibiotics [1]. Constant use of antibiotics by humans both as a medical treatment as well as a drug in other industries (such as farm animal industry) has enabled a population growth of antibiotic-resistant bacteria in the environment [2]. New methods of treatment must be developed in order to combat this threat.

The 16S ribosomal RNA of *E. Coli* is responsible for translation of proteins that are key to the bacteria's function and is often targeted in order to treat bacterial infections. Common antibiotics such as paromomycin and neomycin B bind to the 16S ribosomal RNA and interfere with translation which ultimately leads to the death of the bacteria [3]. There are many ways that antibiotic-resistant bacteria have developed immunities to these aminoglycoside antibiotics. Simple base pair mutations in the structure of the 16S-rRNA can inhibit antibiotics from being able to bind due to structural changes [3]. Efflux pumps are proteins in bacteria that can rapidly pump antibiotics out of the cell [4]. Other antibiotic-resistant bacteria are able to enzymatically deactivate antibiotics or are impermeable to certain antibiotics [5; 6]. Novel drugs that are able to bypass these defensive mechanisms and target the 16S-rRNA are of great importance in order to treat infections that are caused by antibiotic-resistant bacteria.

Using specific peptides to target the 16SrRNA of *E. coli* is a possible answer to overcoming bacterial defense mechanisms. The peptide HPVHHYQ has been shown to bind to 16S ribosomal RNA with a moderate binding affinity (K_D = 16 μM) and the peptide LPLTPLP

has also been shown to have selectivity for 16S-rRNA via an on-bead fluorescence assay [7]. The peptide WRWYCR has also been shown to have antimicrobial activity by affecting several iron regulatory proteins; such that iron levels reach a high level of toxicity in the bacteria and the ferric uptake regulatory protein is unable to bind free iron [8]. WRWYCR is also able to inhibit formation of a Holliday junction in bacteria compromising the ability for genetic recombination [8]. The shiga toxin-producing *E. Coli* mentioned above has also been shown to be effectively treated by peptide WRWYCR [1].

Artificial nuclease derivatives of these peptides were synthesized and cleavage of fluorescein labeled 16S ribosomal RNA was studied. These copper bound peptides are part of a family of metal chelates previously studied by the Cowan lab which are shown to bind and transport reactive metal centers to active sites of nucleic acids [9; 10]. RNA cleavage reactions were carried out using both copper bound peptides, non copper bound GGHGWRWYCR, and free Cu under oxidative and non-oxidative conditions. Rates of reaction were determined through the analysis of time dependent reactions by use of PAGE and MALDI-TOF mass spectrometry.

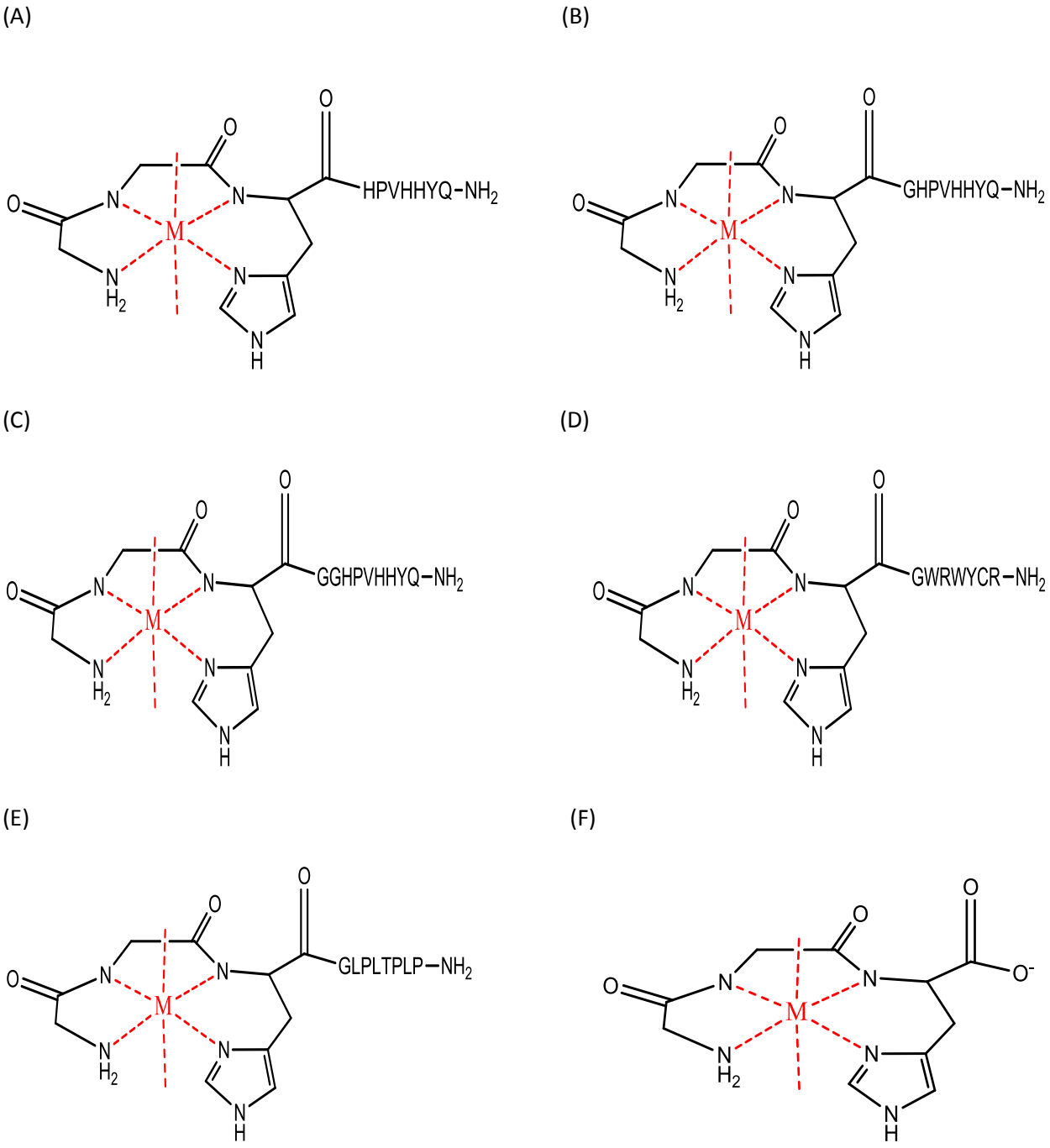

Figure 1. Summary of copper peptide complexes studied. The binding of copper (M) is shown at the GGH terminal end of the peptides. (A) Cu-GGHHPVHHYQ, (B) Cu-GGHGHPVHHYQ, (C) Cu-GGHGGHPVHHYQ, (D) Cu-GGHGWRWYCR, (E) Cu-GGHGLPLTPLP, (F) Cu-GGH

Materials

Fluorescein labeled 16S-rRNA with sequence Fl-GGCGUCACACCUUCGGGUGAAG-UCGCC was purchased from Dharmacon. Peptides GGHHPVHHYQ, GGHGHPVHHYQ, GGHGGHPVHHYQ, GGHGWRWYCR, and GGHGLPLTPLP were purchased from Genemed Synthesis Inc, while peptide GGH was purchased from Bachem. Both RNA and peptides were immediately aliquoted into single use containers and stored at -20° C to minimize freezing and thawing the reagents. Sodium chloride, hydrogen peroxide, and sodium hydroxide were purchased from Fisher, and HEPES was purchased from Sigma. Ascorbate was purchased from Fluka. Ni(II) tetrahydrate and Cu(II) chloride were purchased from Aldrich and J.T. Baker respectively. C_{18} zip-tips and acetonitrile were obtained from Millipore and Fisher, respectively. Matrix components ammonium citrate and 3-hydroxypicolinic acid were obtained from Aldrich and Sigma-Aldrich, respectively.

Methods

Characterization

Peptides were assumed to have purity provided on the manufacturer's label and were dissolved in H_2O to an estimated concentration of 10 mM. Titrations were then performed using 500 μL of estimated 100 μM peptides, titrating with 1 mM Ni(II) tetrahydrate. UV/Vis spectroscopy was used to detect absorbance peaks correlating to Ni-GGH at 245 nm and 430 nm. The end point of the titration was then determined in order to calculate the concentrations of the peptides. Peptides were bound to copper at a 1.5:1 ratio and allotted a time period of 30 min to allow complete binding of the copper.

Polyacrilamide Gel Electrophoresis (PAGE)

Time dependent RNA cleavage reactions were performed with 10 μM Fl-16S-rRNA, 10 μM Cu:Peptide, 1 mM H_2O_2, and 1 mM ascorbate in separate tubes, each containing 20 μL of total volume, at 37° C. A 20 mM HEPES and 100 mM NaCl buffer at pH 7.4 was used for all reactions. The Fl-16S-rRNA was heated to 90° C for 5 min and allowed to refold at 37° C before the reactions were started. Reaction tubes were incubated together with Fl-16S-rRNA in a dark incubator and reaction starting times were staggered. Reactions were incubated up to 8 hours and 2 μL of the product mixture was quenched with 998 μL of a 1× Tris-EDTA-acetic acid buffer, 8 M urea, 20 mM HEPES, and 100 mM NaCl, then heated to 90° C again. The remaining 18 μL of the product mixture were placed onto ice for MALDI-TOF MS analysis. Then 5 μL from each quenched reaction tube were loaded into a 10% polyacrilamide 8 M urea gel, such that each gel lane contained 0.1 pmol of Fl-RNA; electrophoresis was performed at 250 V for 1 hour. RNA bands were visualized by using a GE Typhoon variable mode imager by exciting the 5'-fluorescein-labeled RNA at 488 nm with a single-pass emission filter at 526 nm. Gel bands were quantified by using the program ImageQuant. Time dependent disappearance of initial Fl-16S-rRNA was fit to a first-order reaction equation using the program Origin, and initial rates and rate constants were determined from the data. Reactions were also carried with only 1 mM ascorbate as a coreactant, as well as no coreactants.

MALDI-TOF MS (Matrix assisted laser desorption/ionization-time of flight mass spectrometry)

Reactions were performed as described above and quenched by immediately placing on ice, followed by desalting and collection of the the Fl-RNA products from the remaining 18 μL

of product mixture, which was set aside for MALDI-TOF MS analysis, by zip-tipping with a C_{18} column. The column was first washed 2 times with 10 μL 50% (by volume) acetonitrile and 50% (by volume) H_2O, then 3 times with 10 μL 2 M triethylamine acetate. The Fl-RNA products were then extracted from the reaction tubes by loading onto zip-tips, washed 3 times with 10 μL 2 M triethylamine acetate, 3 times with 10 μL H_2O, and then subsequently eluted into 5 μL 50% (by volume) acetonitrile and 50% (by volume) H_2O at 0° C.

MALDI-TOF MS Analysis

Eluted Fl-16S-rRNA products were then mixed with 2.5 μL of a matrix solution containing 42 mg/mL 3-hydroxy picolinic acid and 6.8 mg/mL ammonium citrate in 30% (by volume) acetonitrile and 70% (by volume) water. A Bruker ground steel 96 target microScout plate was pre-spotted with 1 μL of the matrix mixture and allowed to dry. Then 2.5 μL of the RNA/matrix mixture was spotted on pre-spotted targets and allowed to dry. Three separate RNA calibration mixtures of Fl-5mer, Fl-IRESSLIV, and Fl-RRE, with molecular weights of 2057.5, 8851.5, and 12172.5 amu, respectively, were spotted onto the plate under these same conditions. These mixtures were used to calibrate the MALDI-TOF mass spectrometer prior to analysis of reaction products. Analysis was performed on a Bruker MicroFlex LRF instrument. Mass spectra obtained were smoothed and peaks were detected by using the Bruker flexAnalysis program. Observed peaks were compared to an expected mass list by the program MassDaddy (Jeff Joyner) and mass peaks were identified within an error of 200 ppm. Peaks that were under 1000 amu were not assigned due to an exceedingly large amount of possible cleavage products that could be present. Other unassigned peaks may have been catalysts or artifactual products that were formed during MALDI-TOF MS analysis.

Results

Characterization

The solutions of estimated 10 mM peptides were determined to not be as pure as estimated (by weight) and have actual lower concentrations. The peptide GGHGHPVHHYQ was determined to have a correction factor of 48.1% such that the original solution was 4.81 mM (rather than 10 mM). The original solution of the peptide GGHGGHPVHHYQ was determined to be 4.94 mM, and similar concentrations were also determined for the remaining peptides.

PAGE Analysis of RNA Cleavage

Copper bound peptides were incubated with Fl-16S-rRNA,with either 1 mM H_2O_2 and 1 mM ascorbate, 1 mM ascorbate, or no coreactants. Control experiments were also performed that lacked catalyst, with either 1 mM H_2O_2 and 1 mM ascorbate, or no coreactants. Reactions were also performed with unbound peptide GGHGWRWYCR in order to compare rates of copper and metal free GGHGWRWYCR. The reactivity of free copper and Cu-GGH was also tested and showed high rates of cleavage of RNA, but only when 1 mM H_2O_2 and 1 mM ascorbate were both present. The rate for each complex was determined by the rate of disappearance of the band of full length RNA visualized by gel electrophoresis. Initial rates of reactions for these complexes are summarized in Tables 1, 2, and 3. The metallopeptides Cu-GGHGWRWYCR, Cu-GGHGHPVHHYQ, and Cu-GGH showed the highest initial rates of RNA cleavage among the copper peptide complexes for reactions with 1 mM H_2O_2/ascorbate and 1 mM ascorbate. Free copper also showed a high initial rate of RNA cleavage. Rates of reaction with 1 mM H_2O_2/ascorbate were significantly faster than rates of reaction with 1 mM

ascorbate, indicating that either the complexes are more reactive under more oxidative conditions, the RNA is less stable under more oxidative conditions, or both. In general hydrolytic reactions showed no cleavage of RNA, except for copper bound and metal free peptide GGHGWRWYCR, which elicited relatively rapid formation of a product band by PAGE analysis.

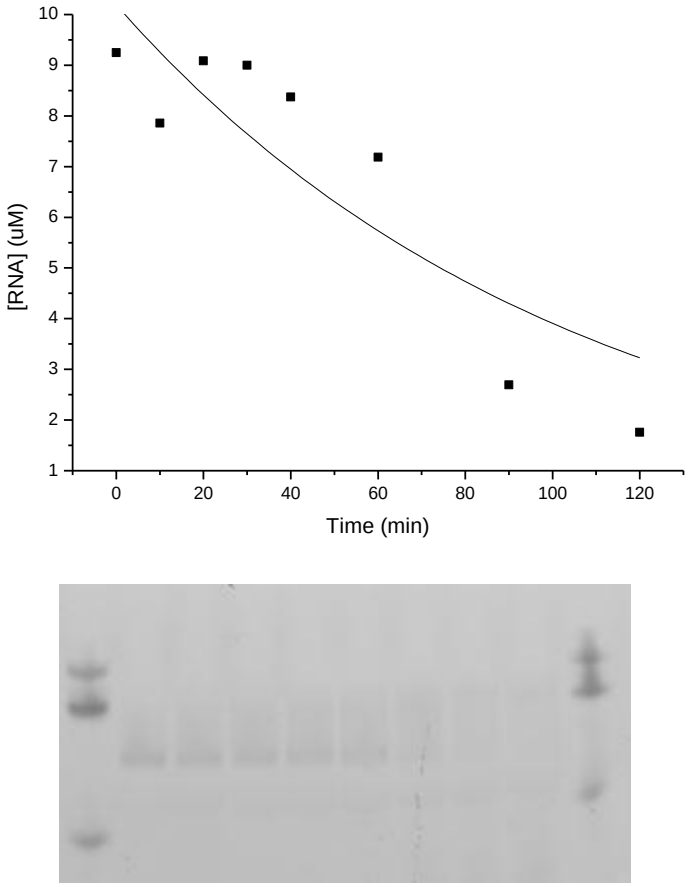

Figure 2. Time dependent cleavage of Fl-16S-rRNA by Cu-GGHGWRWYCR with coreactants hydrogen peroxide and ascorbate. (Top) Disappearance of full-length RNA monitored by PAGE, (Bottom) Gel image showing disappearance of full-length RNA between RNA ladders.

MALDI-TOF MS Analysis of RNA Cleavage

Copper-bound peptides were incubated with Fl-16S-rRNA, with either 1 mM H_2O_2 and 1 mM ascorbate or no coreactants. Control experiments were also performed under all of these conditions. RNA product mixtures were desalted using C_{18} zip-tips and analyzed by MALDI-TOF MS. Products resulting from single-cleavage events were analyzed using the program MassDaddy, which compares observed MS peaks to an expected mass list, containing expected masses for RNA cleavage products. The automation was necessary due to the large amount of data that need to be organized for every time point of every RNA cleavage reaction. The RNA cleavage products that were studied were fragments containing one of 6 easily identifiable nascent overhangs; 3'-hydroxyl , 2',3'-cyclic phosphate, 3'-phosphate, 3'-phosphoglycolate, 5'-hydroxyl, and 5'-phosphate. It was necessary for the expected mass list to contain unique masses for RNA fragments corresponding to all possible RNA modifications at every position along the 16S-rRNA sequence. In this way it was also made possible to approximate cleavage rates along the RNA sequence by using mass spectrometry. Identified peaks can be seen in Figures 3, 4, 5, and 6. By monitoring the increasing peak area fractions of these products over time it was possible to identify that products were formed due to Cu-peptide cleavage and not formed due to artifactual cleavage caused by MALDI-TOF MS. Relative rates of formation of separate cleavage products, as well as disappearance of full-length RNA, were measured over time and used to determine apparent initial rates of RNA cleavage (Tables 1, 2, and 3), as discussed later.

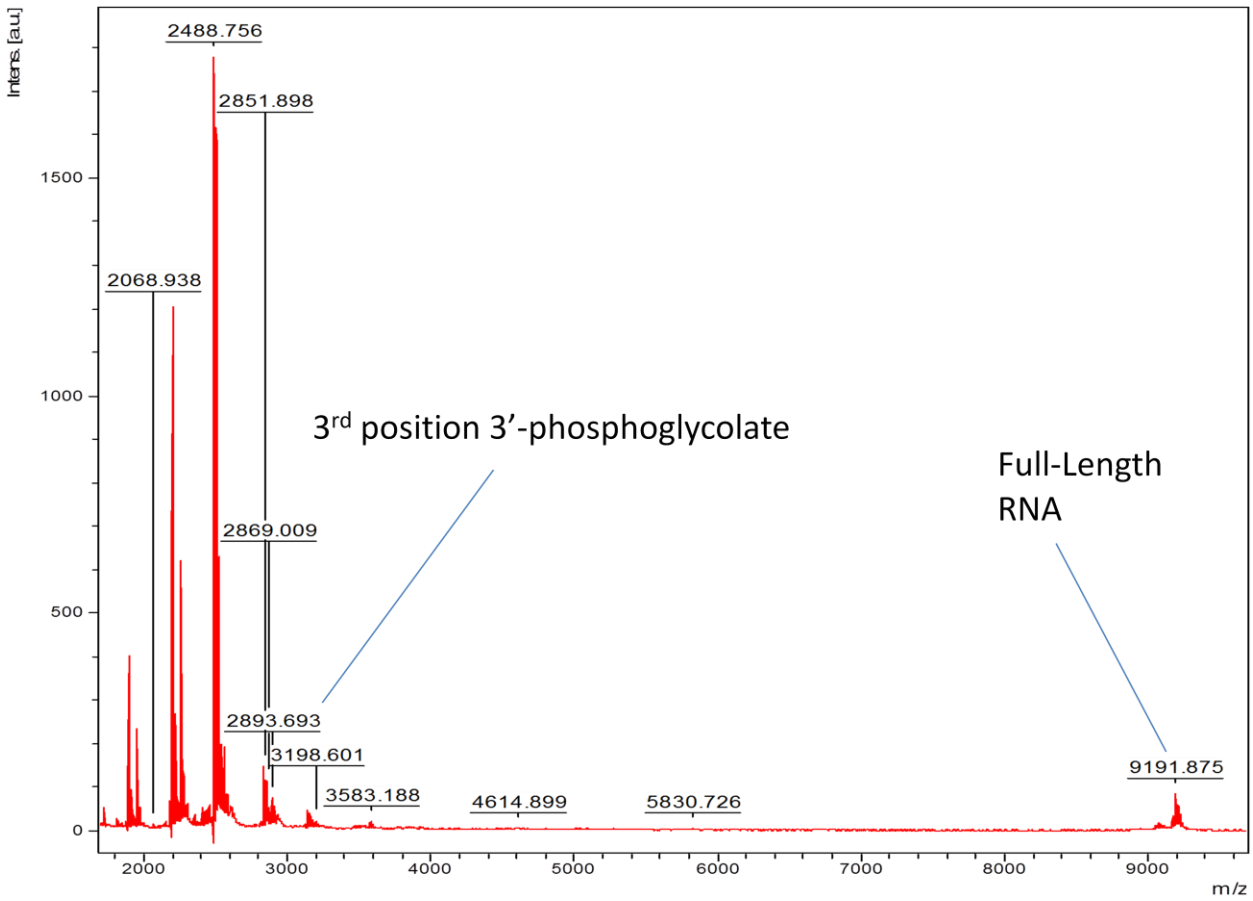

Figure 3. Mass Spectrum of RNA cleavage by Cu-GGHGWRWYCR with 1 mM H_2O_2 and 1 mM ascorbate at 120 min.

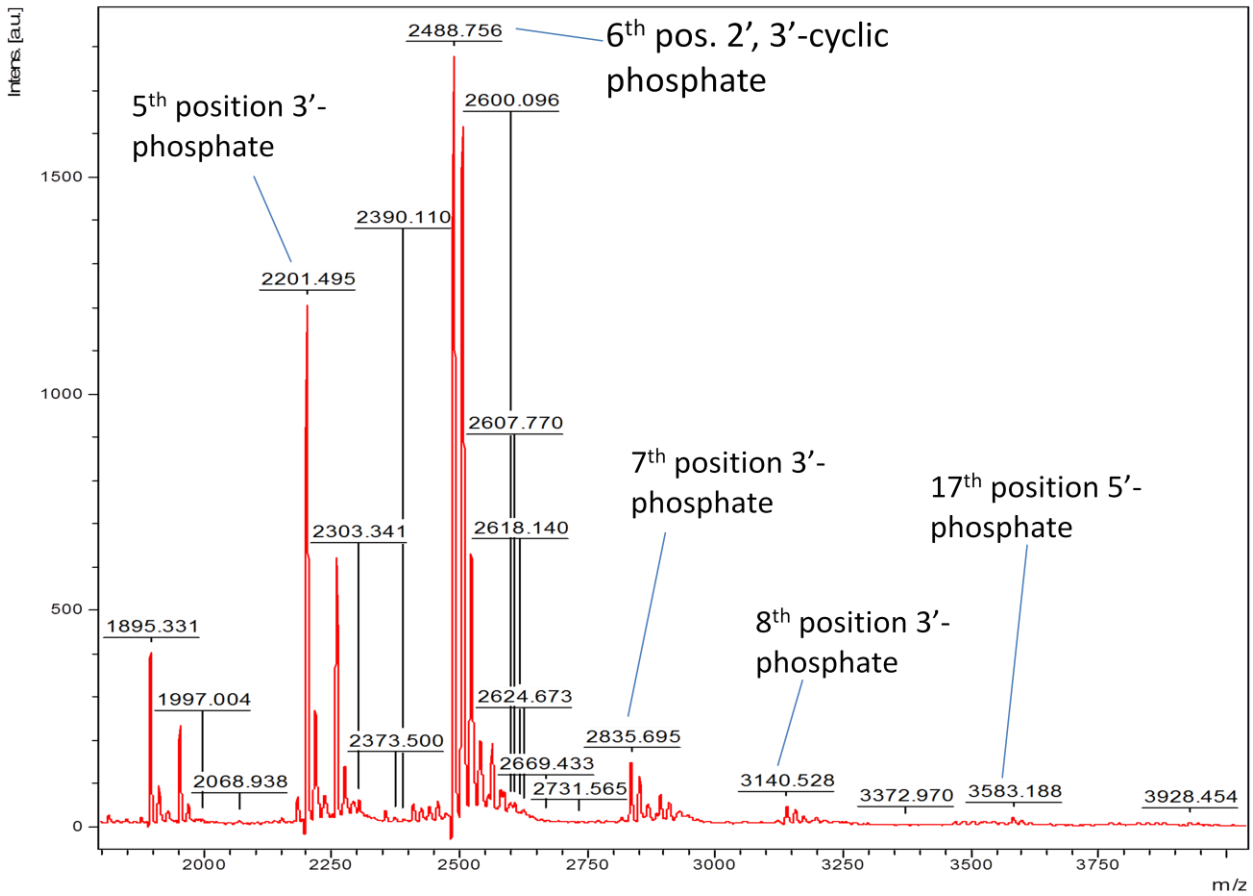

Figure 4. Zoomed Mass Spectrum of RNA cleavage by Cu-GGHGWRWYCR with 1 mM H_2O_2 and 1 mM ascorbate at 120 min.

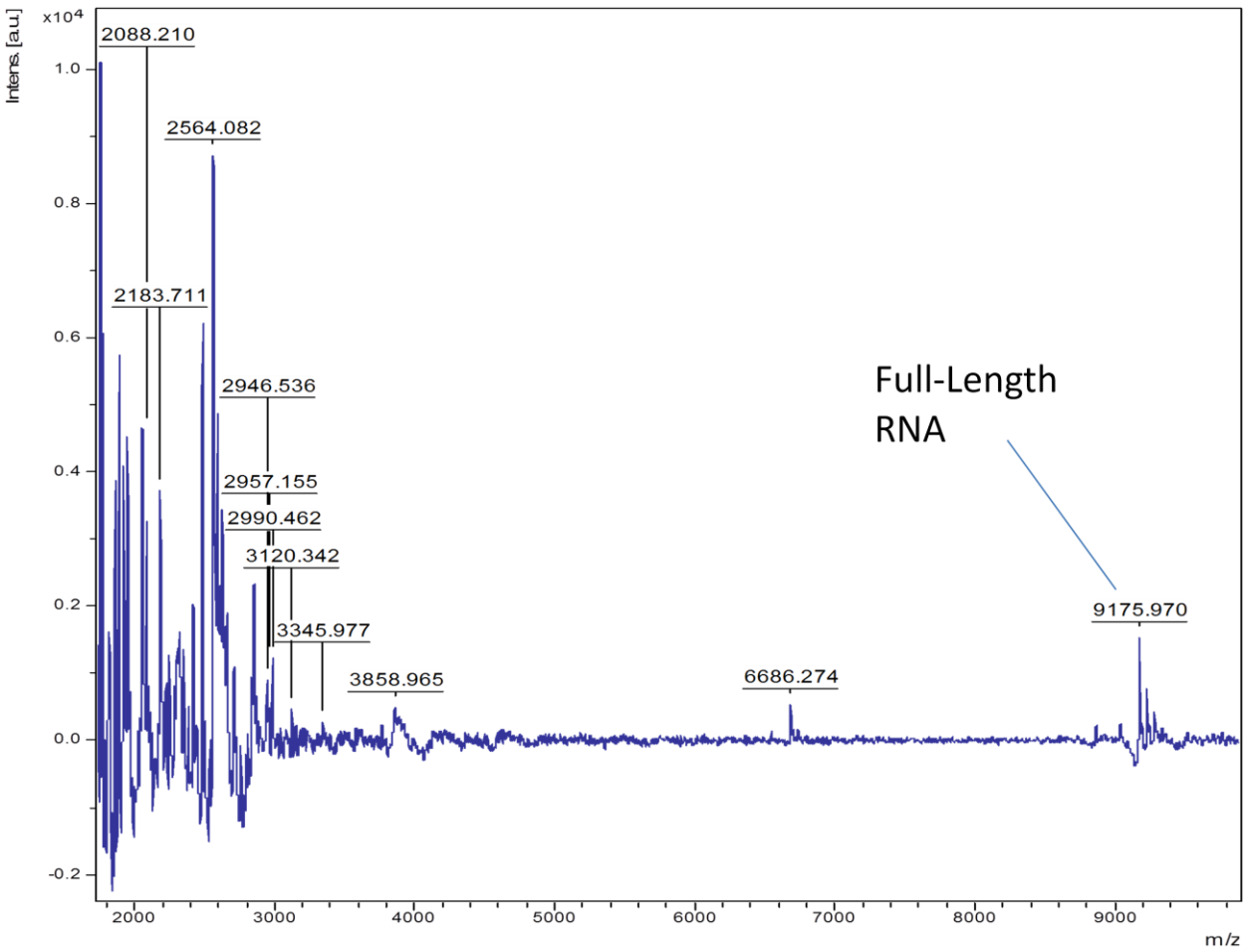

Figure 5. Mass Spectrum of RNA cleavage by GGHGWRWYCR with no coreactants at 6 hr.

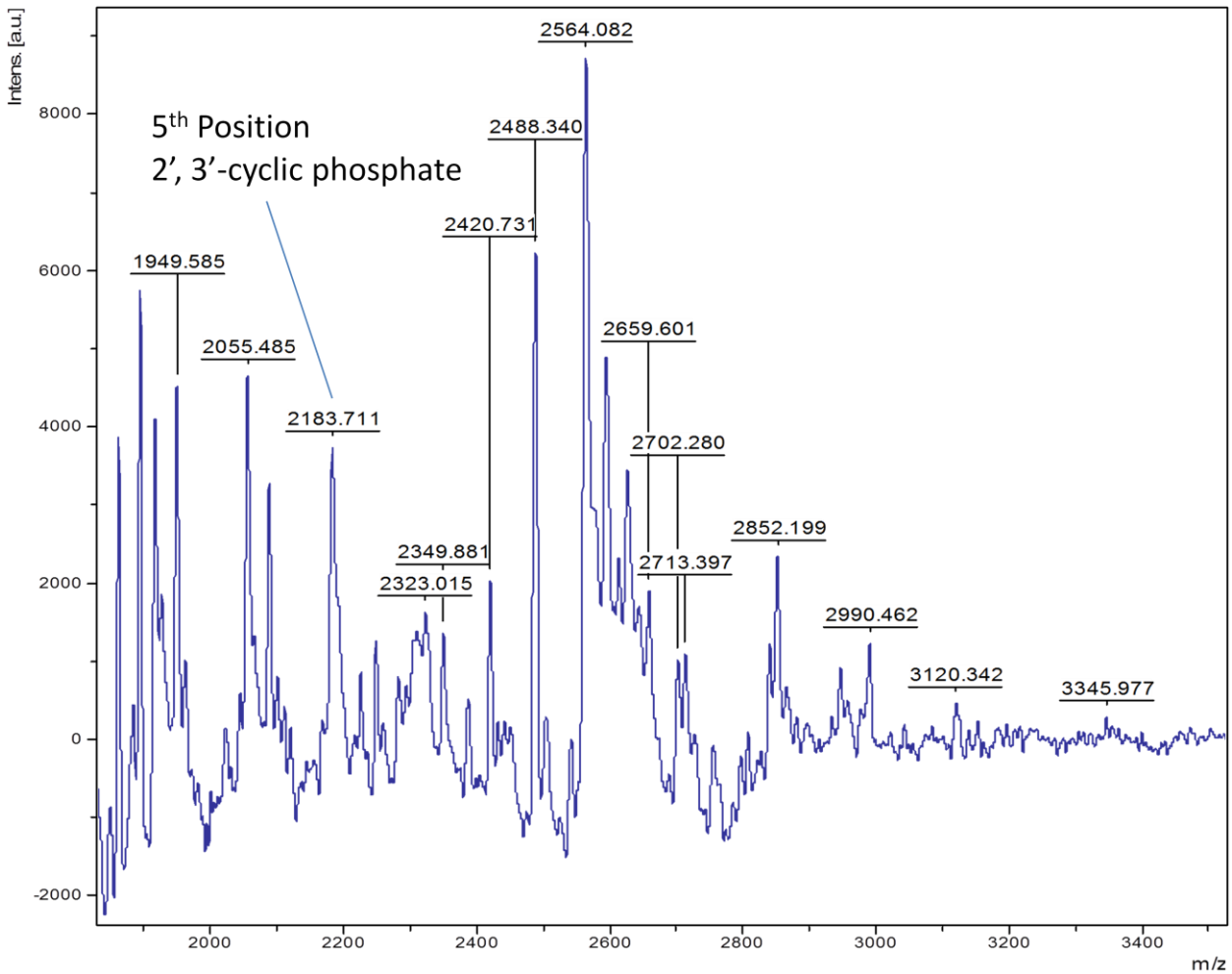

Figure 6. Zoomed Mass Spectrum of RNA cleavage by GGHGWRWYCR with no coreactants at 6 hr.

Table 1. Initial rates of cleavage of 10 μM Fl-16S-rRNA by 10 μM Cu-peptides with 1 mM H_2O_2 and 1 mM ascorbate.

Complex	**PAGE Analysis**	**MALDI-TOF MS Analysis**
	Fl-RNA cleavage (nM/min)	apparent Fl-RNA cleavage rate (nM/min)
Cu-GGHGHPVHHYQ	120 ± 20	45
Cu-GGHGGHPVHHYQ	30 ± 20	63
Cu-GGHGLPLTPLP	< 10	0.1
Cu-GGHGWRWYCR	100 ± 30	97
Cu-GGHHPVHHYQ	1 ± 7	13
Cu-GGH	150 ± 20	160
Free Cu(II)	900 ± 100	530
no complex	5 ± 8	10

Table 2. Initial rates of cleavage of 10 μM Fl-16S-rRNA by 10 μM Cu-peptides with 1 mM ascorbate.

Complex	**PAGE Analysis**	**MALDI-TOF MS Analysis**
	Fl-RNA cleavage (nM/min)	apparent Fl-RNA cleavage rate (nM/min)
Cu-GGHGHPVHHYQ	2 ± 10	n.d.
Cu-GGHGGHPVHHYQ	0 ± 7	n.d.
Cu-GGHGLPLTPLP	0 ± 10	n.d.
Cu-GGHGWRWYCR	1.4 ± 0.2	n.d.
Cu-GGHHPVHHYQ	0 ± 6	n.d.
Cu-GGH	70 ± 10	n.d.
Free Cu(II)	n.d.	n.d.
no complex	n.d.	n.d.

Table 3. Initial rates of cleavage of 10 μM Fl-16S-rRNA by 10 μM Cu-peptides with no coreactants.

Complex	**PAGE Analysis**	**MALDI-TOF MS Analysis**
	Fl-RNA cleavage (nM/min)	apparent Fl-RNA cleavage rate (nM/min)
Cu-GGHGHPVHHYQ	0.00 ± 0.07	10.7
Cu-GGHGGHPVHHYQ	0.3 ± 0.2	8.8
Cu-GGHGLPLTPLP	0.07 ± 0.07	9.5
GGHGWRWYCR	2.4 ± 0.5	14.4
Cu-GGHGWRWYCR	2 ± 2	33.1
Cu-GGHHPVHHYQ	0.1 ± 0.1	8.9
Cu-GGH	0.2 ± 0.5	10.1
Free Cu(II)	0.2 ± 0.7	10.7
no complex	0 ± 0.1	12

*****n.d.: These rates have not been determined.

Discussion

Characterization of Peptides

It was very important to determine the exact concentration of the peptides in order to ensure that there was enough peptide in the Cu-peptide complex mixtures. If there was not enough peptide to bind all of the copper, then cleavage of the RNA would not have only been the result of the metallopeptide, but also that of free copper which would have complicated the cleavage data.

PAGE Analysis of RNA Cleavage Kinetics

Reactions containing the oxidative coreagents, 1 mM H_2O_2 and 1 mM ascorbate, generally showed higher initial rates of RNA cleavage, while most metallopeptides were unreactive under hydrolytic conditions with no coreactants. However, a notable exception was observed for Cu-GGHGWRWYCR and GGHGWRWYCR, and will be discussed later.

The Cu-peptide complexes Cu-GGHGHPVHHYQ and Cu-GGHGWRWYCR showed the highest initial rates of RNA cleavage among the Cu-peptide complexes, with their initial rates with 1 mM H_2O_2 and 1 mM ascorbate being 120 nM/min and 100 nM/min respectively. The peptide GGHGHPVHHYQ is part of the family of peptides in this study that contains the HPVHHYQ peptide known to target 16S-rRNA. This specific peptide most likely has a higher initial rate of cleavage than the other HPVHHYQ-derived peptides due to the single glycine linker connecting the peptide to the terminal copper binding GGH sequence. This single linker most likely allows the catalyst to attain a more favorable structure and/or alignment with respect to the Fl-16SrRNA promoting faster cleavage under oxidative conditions.

Cu-GGH and free copper also had high initial rates of RNA cleavage, this could be due to a copper binding site on the 16SrRNA, allowing these complexes to bind tightly to the RNA and effect cleavage. Also, these catalysts may be more reactive with the coreactants, causing a greater production of reactive oxygen species that cause cleavage of the RNA [8].

MALDI-TOF MS Analysis of RNA Cleavage Kinetics

The peak area fractions for each species at each time point were used in order to determine apparent initial rates for each complex studied. All observed peak areas output by MassDaddy for one time point were summed together, and each individual peak area was divided by this sum in order to obtain peak area fractions. Apparent mole fractions were then estimated from these peak area fractions and used to calculate the apparent initial rates of cleavage. This method has limitations because it does not take into account all the peaks in any mass spectrum that are products from the RNA. There is also a bias on the size of the molecules detected, since larger molecules are not as readily detected as smaller ones by mass spectrometry [11]. Also peaks that were below an m/z of 1000 were not analyzed because of the complication of identifying RNA products resulting from multiple cleavage events.

Comparison of PAGE to MALDI-TOF MS

With the limitations previously stated that MALDI-TOF MS present when attempting to determine initial rates of RNA cleavage it is not surprising to find that rates between PAGE and MALDI-TOF analysis do not completely agree. With this being said, however, many of the MALDI-TOF initial rates do strongly support the PAGE analysis, as can be seen with the initial RNA cleavage by Cu-GGHGWRWYCR and Cu-GGH with 1 mM H_2O_2 and 1 mM ascorbate

(Table 1). In general, MALDI-TOF MS apparent initial rates of RNA cleavage are able to support PAGE data to a certain extent, since the determined rates are within the same magnitude.

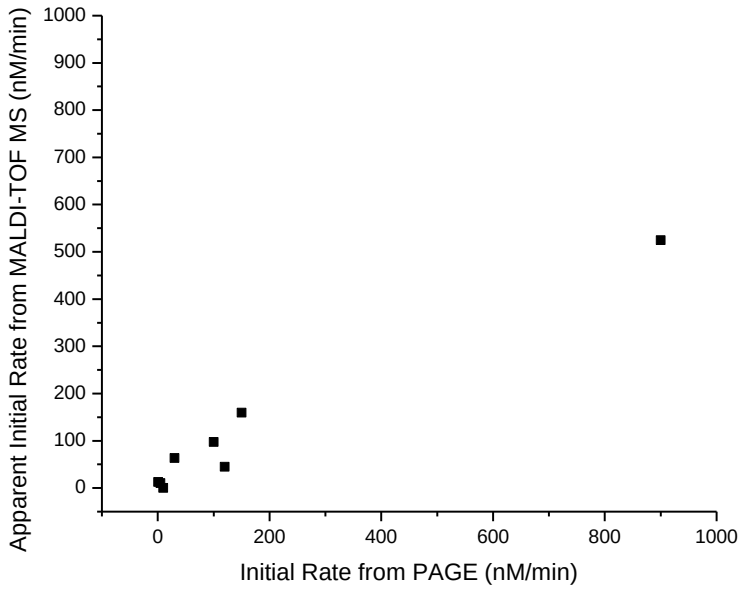

Figure 7. Plotted initial rates of RNA cleavage determined by MALDI-TOF MS vs. PAGE for each catalyst with 1 mM H_2O_2 and 1 mM ascorbate.

Activity of WRWYCR

Previous studies have shown that peptide WRWYCR is an antimicrobial agent through a handful of proposed mechanisms [8]. WRWYCR interferes with the correct function of the ferric uptake regulatory protein and also inhibits genetic recombination in bacteria by interfering with the regular processing of Holliday junctions [8, 12]. Our study shows that these may not be the only mechanisms of antimicrobial activity for peptide WRWYCR. Under hydrolytic conditions the peptide GGHGWRWYCR and metallopeptide Cu-GGHGWRWYCR were able to cleave Fl-16S-rRNA. Only these catalysts showed product formation by PAGE analysis. MALDI-TOF MS analysis of Cu-GGHGWRWYCR and GGHGWRWYCR showed formation

of 2, 3'-cyclic phosphate at position 5 along the RNA (Figure 8 and 9), indicating that these catalysts promote nucleophilic attack by the 2'-O to nearby phosphate group [13]. Other catalysts showed no major products as can be seen in Figure 10. Cleavage by metallopeptides with coreactants 1 mM H_2O_2 and 1 mM ascorbate showed a wider distribution of product formation, showing 2', 3'-cyclic phosphate, 3'-phosphate, and 3'-phosphoglycolate as major products (Figure 11). This study proposes that the antimicrobial activity of peptide WRWYCR may be due not only to its inhibition of iron regulation and Holliday junctions, but also due to its ability to cleave the 16S ribosomal RNA of *E. coli*. The ability for these catalysts to cleave the Fl-16S-rRNA is interesting, since it shows that the catalysts have unique activity that degrades the RNA. This likely makes WRWYCR an ideal candidate for antibacterial use, since it displays several mechanisms by which it could possibly have antimicrobial activity. Antibiotic-resistant bacteria would have to be resistant to all of the antimicrobial activity of WRWYCR in order to survive treatment.

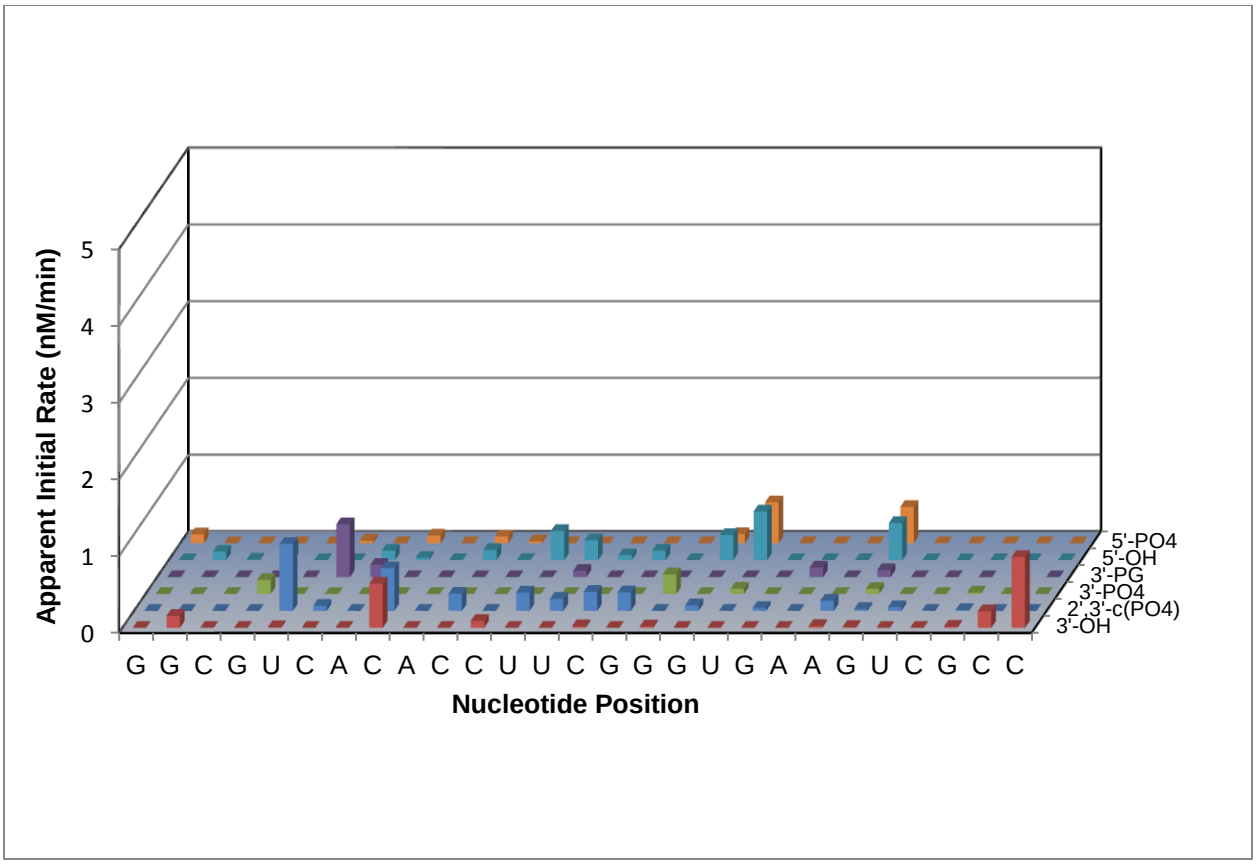

Figure 8. Apparent initial rates of formation of several cleavage products from reaction of Fl-16S-rRNA with Cu-GGHGWRWYCR and no coreactants.

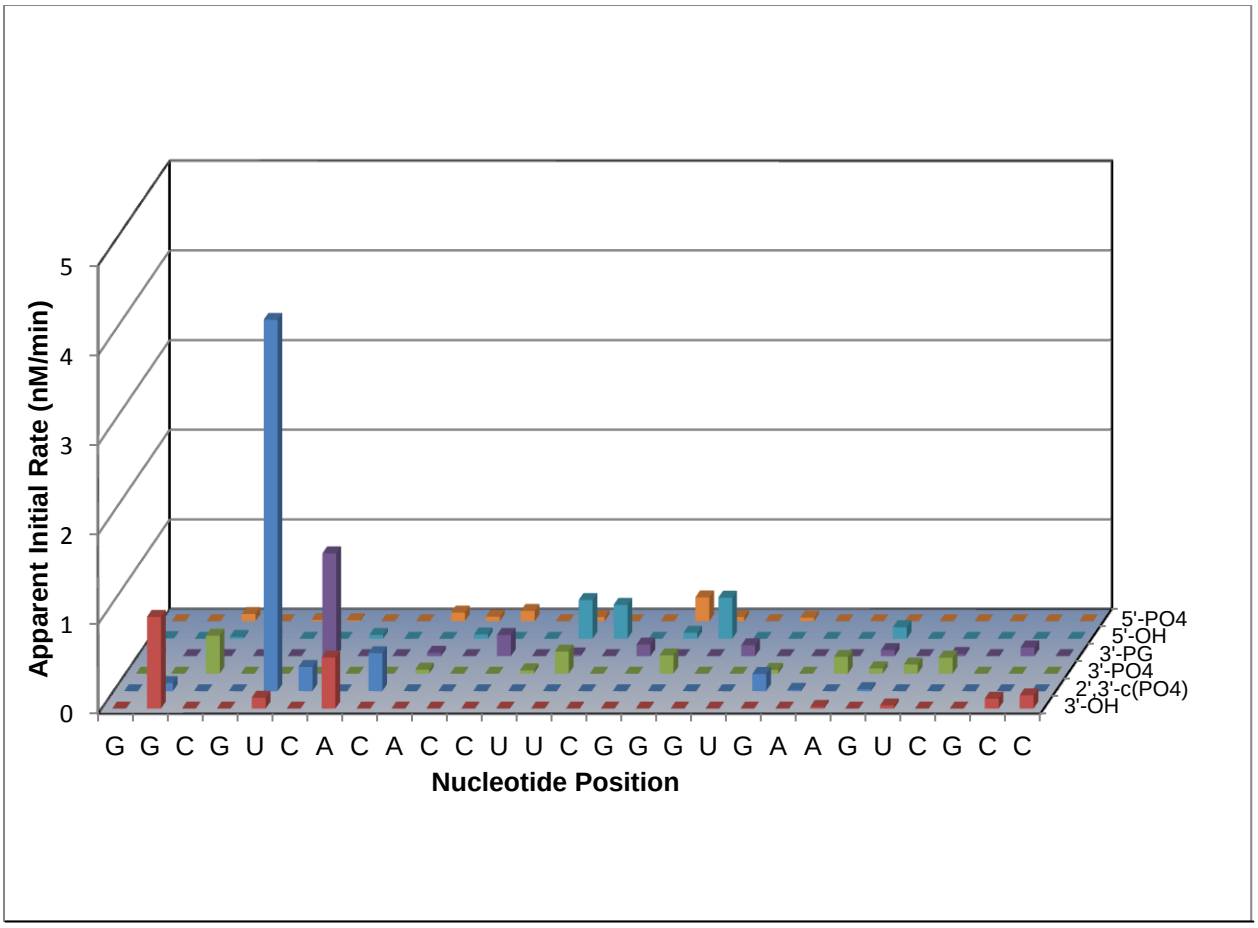

Figure 9. Apparent initial rates of formation of several cleavage products from reaction of Fl-16S-rRNA with GGHGWRWYCR and no coreactants.

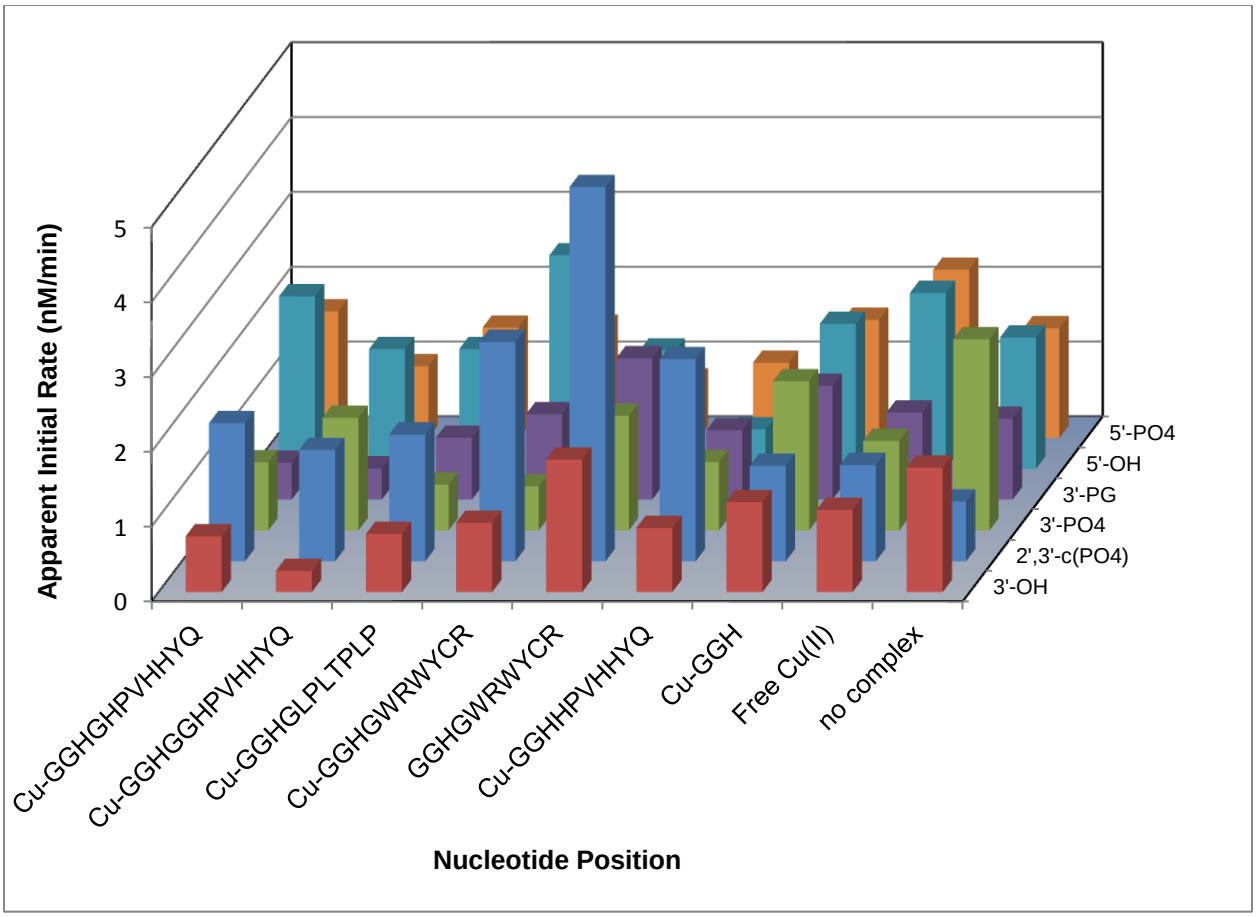

Figure 10. Apparent initial rates of formation of several cleavage products from reaction of Fl-16S-rRNA with every catalyst and no coreactants.

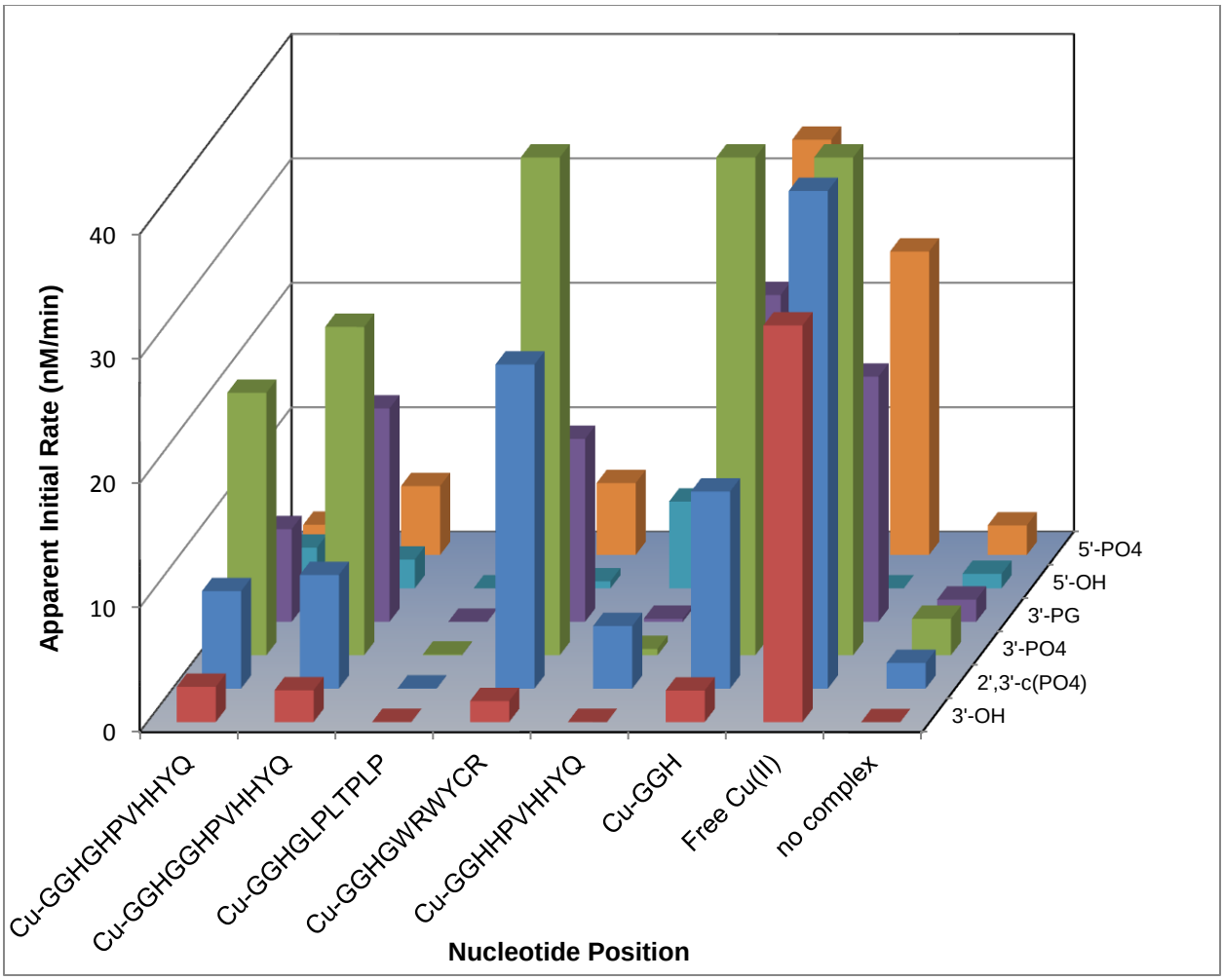

Figure 11. Apparent initial rates of formation of several cleavage products from reaction of Fl-16S-rRNA with every catalyst, 1 mM H_2O_2, and 1 mM ascorbate.

Conclusions

This study shows effective cleavage of the Fl-16S-rRNA by several Cu-peptide complexes and the products formed. Metallopeptides based off of the HPVHHYQ peptide showed effective cleavage of the Fl-16S-rRNA. Cu-GGHGHPVHHYQ showed the highest rates of cleavage, possibly due to its single glycine linker lending it a more favorable structure to bind to the RNA. Cu-GGHGWRWYCR and GGHGWRWYCR were able to cleave the Fl-16SrRNA under all conditions, including under hydrolytic conditions with and without copper bound to it. MALDI-TOF MS analysis shows that these two catalysts promote cleavage of the RNA in order to form a 2', 3'-cyclic phosphate at the 5^{th} position along the RNA. Cleavage by these two catalysts is interesting because it shows another possible mechanism by which the peptide WRWYCR may show antimicrobial activity. With antibiotic-resistant bacteria becoming more prevalent, new treatments need to be developed that are able to overcome the mechanisms bacteria have developed. Peptide WRWYCR is unique because it displays characteristics of several mechanisms of antimicrobial activity. This makes this peptide ideal for study because it could possibly be used to effectively treat several different kinds of bacteria, even those that have developed multiple defense mechanisms.

References

[1] M. Lino, J.V. Kus, S.L. Tran, Z. Naqvi, B. Binnington, S.D. Goodman, A.M. Segall and D.B. Foster, A novel antimicrobial peptide significantly enhances acid-induced killing of Shiga toxin-producing *Escherichia Coli* O157 and non-O157 serotypes. Microbiology. 157 (2011) 1768-1775.

[2] D. Maura and L. Debarbieux, Bacteriophages as twenty-first antibacterial tools for food and medicine. Appl. Microbiol. Biotechnol. 90 (2011) 851-859.

[3] D. Fourmy, M.I. Recht, S.C. Blanchard, and J.D. Puglisi, Structure of the A Site of Escherichia coli 16S Ribosomal RNA Complexed with an Aminoglycoside Antibiotic. Science. 274 (1996) 1367-1371.

[4] N.A. Villagra, J.A. Fuentes, M.R. Jofré, A.A. Hidalgo, P. García, and G.C. Mora, The carbon source influences the efflux pump-mediated antimicrobial resistance in clinically important Gram-negative bacteria. J. Antimicrob. Chemother. 67 (2012) 921-927.

[5] P.G. Young, R. Walanj, V. Lakshmi, L.J. Byrnes, P. Metcalf, E.N. Baker, S.B. Vakulenko, and C.A. Smith, The Crystal Structures of Substrate and Nucleotide Complexes of *Enterococcus faecium* Aminoglycoside-2”-Phosphotransferase-IIa [APH(2”)-IIa] Provide Insights into Substrate Selectivity in the APH(2”) Subfamily. J. Bacteriol. 194 (2012) 4133-4143.

[6] E. Eren, J. Vijayaraghavan, J. Liu, B.R. Cheneke, D.S. Touw, B.W. Lepore, M. Indic, L. Movileanu, and B. van den Berg, Substrate Specificity within a Family of Outer Membrane Carboxylate Channels. PLoS Biol. (2012)

[7] M. Li, A.C.E Duc, E. Klosi, S. Pattabiraman, M.R. Spaller, and C.S. Chow, Selection of Peptides That Target the Aminoacyl-tRNA Site of 16S Ribosomal RNA. Biochemistry. 48 (2009) 8299-8311.

[8] S.S. Orchard, J.E. Rostron, A.M. Segall, *Escherichia coli* enterobactin synthesis and uptake mutants are hypersensitive to an antimicrobial peptide that limits the availability of iron in addition to blocking Holliday junction resolution. Microbiology. 158 (2012) 547-559.

[9] J.C. Joyner and J.A. Cowan, Targeted Cleavage of HIV RRE RNA by Rev Coupled Transition Metal Chelates. J. Am. Chem. Soc. 133 (2011) 9912-9922.

[10] J.C. Joyner, K.D. Keuper, and J.A. Cowan, DNA Nuclease Activity of Rev-Coupled Transition Metal Chelates. Dalt. Trans. (2012).

[11] S.J. Wetzel, C.M. Guttman, J.E. Girard, The influence of matrix and laser energy on the molecular mass distribution of synthetic polymers obtained by MALDI-TOF-MS. Int. J. Mass spectrom. 238 (2004) 215-225.

[12] M.C. Rideout, J.L. Boldt, G. Vahi-Ferguson, P. Salamon, A. Nefzi, J.M. Ostresh, M. Giulianotti, C. Pinilla, and A.M Segall. Potent antimicrobial small molecules screened as inhibitors of tyrosine recombinases and Holliday junction-resolving enzymes. Mol. Divers. 15 (2011) 989-1005.

[13] S. Gwiazda, K. Salomon, B. Appel, and S. Müller. RNA self-ligation: From oligonucleotides to full length ribozymes. Biochimie. (2012)